Journal of Marine Research, 51, 771–795, 1993

The splitting of eddies along boundaries

by Chuan Shi[1,2] and Doron Nof[3]

ABSTRACT

This paper addresses the question of what happens to an eddy that is forced "violently" against a boundary by, say, an advective current or another vortex. The detailed temporal evolution of such a collision on an f-plane is examined using a barotropic, as well as a one-and-a-half-layer contour dynamics model with surgery procedures. Both the barotropic eddy and the one-and-a-half-layer eddy initially have two circular potential vorticity fronts: an inner front at which the velocity increases to a maximum from zero at its center, and an outer front (e.g., the edge of the eddy) at which the velocity reduces to zero.

At $t = 0$, the circular eddy is conceptually cut off by the wall. It is demonstrated that such a cut corresponds to the violent forcing of the eddy against the wall. One intuitively expects that, as a result of the collision, the eddy would simply leak fluid along the wall (forming a thin jet) until it shrinks to such a size that it is merely "kissing" the wall (Nof, 1988a). In contrast to this intuition, however, it is found that, after the eddy is cut by the wall (i.e., $t > 0$), the annulus fluid (i.e., the fluid between two fronts) is gradually advected along the wall forming a *new eddy* next to the interior (i.e., the region inside the inner front). After formation, both the off-spring eddy and the parent eddy migrate along the wall away from each other. This migration is mainly due to the image effect that is created by the wall and separates the eddies even farther. As time goes on, the migration intensifies because the mutual advection of the eddies forces them farther into the wall so that the image effect increases.

These results of our contour dynamics study are in good agreement with additional experiments of an isopycnic, primitive equation model. Namely, both of these studies illustrate that an eddy-wall collision causes the parent eddy to split into two migrating eddies, one that contains the core of the parent and the other that contains fluid from the rim.

Possible applications of these models to eddies pushed against the shelf in the Gulf of Mexico are discussed.

1. Introduction

Interaction between eddies and boundaries is inevitable because of two processes. First, the variation of the Coriolis parameter with latitude forces eddies toward the western boundaries of the ocean. Second, advection by main currents or propulsion

1. Department of Oceanography B-169, The Florida State University, Tallahassee, Florida, 32306-3048, U.S.A.

2. Present address: Horn Point Environmental Laboratory, Center for Environmental and Estuarine Studies, University of Maryland, Cambridge, Maryland, 21613-0775, U.S.A.

3. Department of Oceanography B-169, and the Geophysical Fluid Dynamics Institute, The Florida State University, Tallahassee, Florida, 32306-3048, U.S.A.

induced by neighboring eddies also force eddies toward the ocean walls. The former process causes a "soft" and "gentle" impact with the western wall because the β-induced westward speed is relatively small [$O(1$ km day$^{-1})$] so that it takes many days [$O(\beta R_d)^{-1}$, where R_d is the Rossby radius] for a significant fraction of the eddy (i.e., a distance comparable to the eddy diameter) to be pushed into the wall. The latter processes, on the other hand, can be of a more "explosive" and "violent" nature as advection [$O(10 - 100$ km day$^{-1})$] can push an eddy into the wall so rapidly that gross distortions in the eddy shape (and structure) can occur in a matter of days. The "gentle" eddy-wall interaction process has been studied extensively in Shi and Nof (1993) and the present article focuses on the more "explosive" and "violent" collision.

Shi and Nof (1993) have shown that a soft collision is typically associated with (i) a small leakage from the eddy rim which forms a thin jet along the wall, and (ii) a transformation of the eddy into a half-circular structure that migrates steadily along the wall (a wodon). We shall show in the present study that a violent collision causes more drastic effects. In particular, the eddy will not only migrate along the wall but will also split into *two* eddies with an opposing sense of rotation.

To do so, we shall use the so-called contour dynamics method, which will be applied to an eddy on an f-plane. At $t = 0$, an eddy is conceptually cut by a wall (as if the advection forced the eddy into the wall). For completeness, we shall also investigate this process using a constant potential vorticity eddy and a Gaussian eddy in an isopycnic model. Note that the contour dynamics method is a Lagrangian approach, whereas the isopycnic model is a Eulerian method. We shall show that both of these studies point to a new counter-intuitive eddy splitting process. We speak here about a counter-intuitive process because intuitively we would expect that an eddy that is cut by a wall would simply leak along the wall until its outer rim leaks out completely and its core is merely "kissing" the wall [see Fig. 1 adapted from Nof, 1988a]. It turns out, however, that such a benign state is never reached and that instead both the core and the leaked fluid are forced farther and farther into the wall.

a. Background

Closely related works are briefly discussed below. In the studies reviewed, the first two address the leaked fluid along the wall. The next three explain how an along-wall current formed an eddy, whereas the last three studies illustrate that eddy-wall collisions generate linear waves.

i. Eddy-wall collisions generating along-wall flows. Nof (1988a,b) considered a barotropic model and a one-and-a-half-layer model to examine the collision of isolated eddies with vertical walls on an f-plane. His case is very similar to that of this study but has quite a severe limitation because it employs a quasi-steady model. In both his barotropic model and the one-and-a-half-layer model, he found that cyclonic (anticyclonic) eddies must leak fluid to the left (right) along the wall (looking off-shore). In

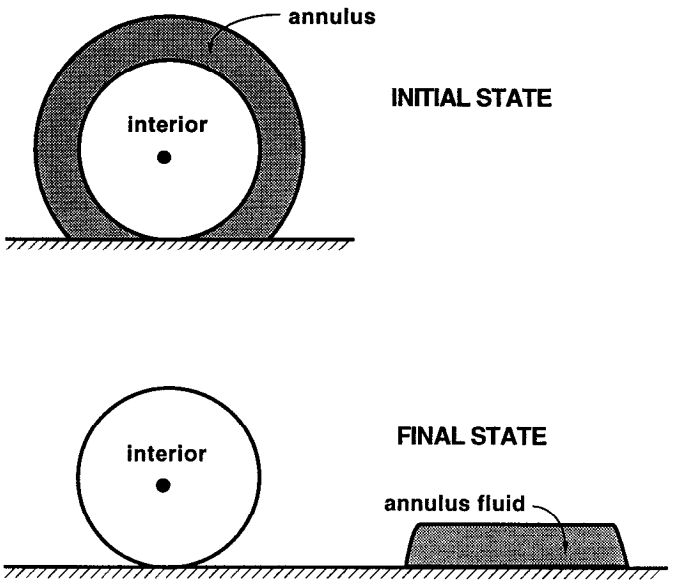

Figure 1. The (intuitively) expected ultimate stage of the eddy-wall interaction according to Nof (1988a). The outer rim of the (anticyclonic) eddy has leaked out and has formed a long narrow strip on the right-hand side. As a result, the vortex has shrunk and is merely touching the wall. We shall see that such a benign state is not reached in "violent" eddy-wall collisions.

his qualitative experiments on a rotating table, he showed that anticyclonic eddies indeed leaked fluid to the right along the wall. Here, Nof's results are extended to a fully time-dependent, nonlinear problem using a contour dynamics model as well as an isopycnic model.

ii. Eddies generated by along-wall flows. In contrast to Nof's studies, Stern and Pratt (1985) pointed out that an along-wall jet could generate an eddy near its nose. They demonstrated that a jet along a wall generated an eddy when a patch of fast-moving fluid caught up with a slower patch. Stern (1986) considered the evolution of a coastal current using a quasi-geostrophic, one-and-a-half-layer, contour dynamics model. Similarly, he found that an eddy was formed near the nose of the coastal current. Stern (1989) studied the evolution of locally unstable barotropic shear flow along a wall by examining the collisions of two vorticity fronts intersecting the wall using a contour dynamics model. He again found that the frontal jet-wall collisions produced a large eddy near the nose of the jet. We shall show that eddy-wall collisions produce an along-wall flow which forms an eddy.

iii. Waves generated by eddy-wall collisions. One intuitively expects eddy-wall collisions to generate waves, and it is, therefore, of interest to review previous studies related to this phenomenon. The earliest are those of Minato (1982; 1983) who

studied the geostrophic adjustment of a warm-core eddy near the wall using a linear, inviscid, one-and-a-half-layer model on an f-plane. He found that the eddy lost parts of its volume and energy due to the generation of internal Kelvin and Poincare waves near a wall. Umatani and Yamagata (1987) studied evolution of an isolated eddy near a wall and discussed the nonlinear Kelvin wave excited during the adjustment process. Dorofeyev and Larichev (1992) studied the collision of a dipole-like eddy with a wall using a linear, barotropic model on a β-plane. They noted an exchange of fluid mass between a geostrophic eddy and an ageostrophic Kelvin wave during collisions of an eddy with a wall.

Though the above studies are informative, they do not directly address the violent time dependent collision process that is of interest in this investigation.

b. Present approach—a contour dynamics and isopycnic model

The contour dynamics method originated from the so-called water-bag model (Berk and Roberts, 1970). In the late 1970s, this water-bag model was imported into the study of classical fluid dynamics problems and then renamed the contour dynamics model. Zabusky *et al.* (1979) first described the basic algorithm behind this contour dynamics model. It can be outlined as follows. A number of Lagrangian points are placed on a vorticity front. The evolution of such Lagrangian points is governed by a set of integro-differential equations, which can be derived from the vorticity or potential vorticity equations. We obtain the positions of all points by numerically solving the integro-differential equations at each time step (Section 2). The Bleck and Boudra (1986) isopycnic model that we shall use (Section 3) was already described in Shi and Nof (1993) and need not be repeated here.

After presenting the various models the results will be discussed and applied to rings in the Gulf of Mexico (Section 4) although many other applications can also be thought of.

2. Contour dynamics computations

a. Formulation of the barotropic model

Consider a barotropic field, which, in nondimensional form, satisfies:

$$\nabla^2\psi = \begin{cases} \omega_1 & 0 \le r < 1 \text{ (interior)} \\ \omega_2 & 1 \le r < b \text{ (annulus)} \\ 0 & b \le r < \infty \text{ (outside)}, \end{cases} \tag{2.1}$$

where ψ is a streamfunction defined by $u = -\partial\psi/\partial y$ and $v = \partial\psi/\partial x$, ω_1 and ω_2 are the vorticities for the interior and the annulus, and b is the initial, dimensionless, outer front radius (Fig. 2). The initial inner front radius is chosen to be unity, and the outer front radius satisfies the condition $b \ge 1$. The boundary condition of no-flow into the wall is:

$$\psi = \text{constant} \qquad \text{at } y = -w, \tag{2.2}$$

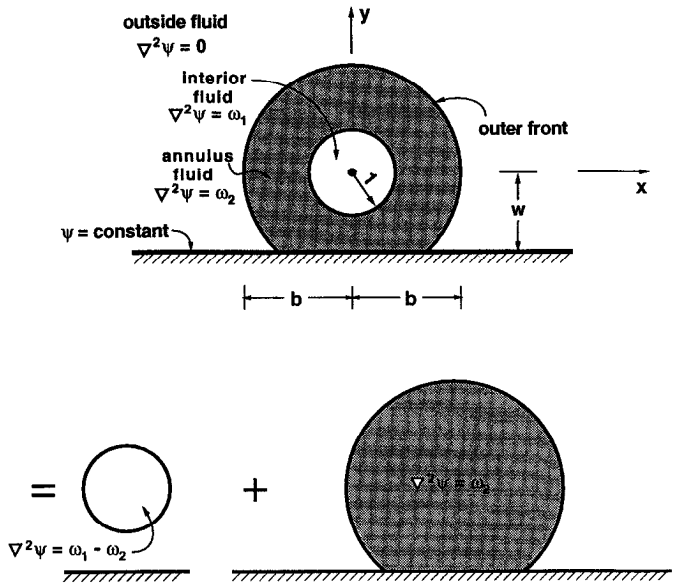

Figure 2. A schematic diagram of "violent" eddy-wall collisions on an f-plane. At $t = 0$, the eddy is conceptually cut by a straight wall; it is demonstrated later that such a cut is equivalent to facing the eddy toward the wall (Fig. 4). There are two vorticity fronts: the inner front and the outer front. These two fronts divide the studied area into three regions: the interior with vorticity ω_1, the annulus with vorticity ω_2, and the outside with no vorticity. For computational convenience, the vorticity of our double connected domain is considered as the sum of the vorticities in two overlapping singly connected domain is domains: the first domain has a vorticity $\omega_1 - \omega_2$, and the second domain has a vorticity ω_2. Our aim is to investigate the subsequent temporal evolution of the two fronts along the wall.

where w is the initial distance between the eddy's center and the wall (Fig. 2). This boundary condition can be satisfied by introducing image vortices in the solution of the Poisson's equation. For simplicity, we choose $\omega_1 = \pm 1$ for the interior and $\omega_2 = -\omega_1/(b^2 - 1)$ for the annulus, so that the eddy's initial circulation is equal to zero without the wall. Under such conditions, the interior vorticity has a sign opposite to that of the annulus vorticity (i.e., $\omega_1\omega_2 < 0$). It will be shown later that the interior vorticity advects the annulus vorticity toward the wall, generating a new eddy (having an opposite sign to the interior vorticity) near the wall.

The corresponding undisturbed azimuthal velocity is

$$v_\theta(r) = \begin{cases} \omega_1 r/2 & 0 \le r \le 1 \text{ (interior)} \\ -\omega_1(b^2 - r^2)/2r(b^2 - 1) & 1 \le r \le b \text{ (annulus)} \\ 0 & b < r < \infty \text{ (outside)}, \end{cases}$$

which, as expected, illustrates that the sign of the interior vorticity is opposite to that of the annulus vorticity. As already mentioned, there are two vorticity fronts: the

inner front at which the velocity reaches maximum, and the outer front at which the velocity decays to zero.

The integrals are evaluated at each point $[x_2(t), y_2(t)]$ on the outer front, and $[x_1(t), y_2(t)]$ on the inner front. For computational convenience, the vorticity of our doubly connected domain is considered as the sum of the vorticities in the two overlapping singly connected domains: the first domain has a vorticity $\omega_1 - \omega_2$, and the second domain has a vorticity ω_2 (Fig. 2). By introducing image vortices to satisfy the boundary condition (2.2), we obtain four coupled, nonlinear, integral-differential equations for the Lagrangian velocities of the two fronts:

$$\frac{dx_1}{dt} = \frac{\omega_2}{4\pi}\oint_o \ln(d_1D_1)\,d\xi + \frac{\omega_1 - \omega_2}{4\pi}\oint_i \ln(d_1D_1)\,d\xi \tag{2.3}$$

$$\frac{dx_2}{dt} = \frac{\omega_2}{4\pi}\oint_o \ln(d_2D_2)\,d\xi + \frac{\omega_1 - \omega_2}{4\pi}\oint_t \ln(d_2D_2)\,d\xi \tag{2.4}$$

$$\frac{dy_1}{dt} = \frac{\omega_2}{4\pi}\oint_o \ln(d_1/D_1)\,d\eta + \frac{\omega_1 - \omega_2}{4\pi}\oint_i \ln(d_1/D_1)\,d\eta \tag{2.5}$$

$$\frac{dy_2}{dt} = \frac{\omega_2}{4\pi}\oint_o \ln(d_2/D_2)\,d\eta + \frac{\omega_1 - \omega_2}{4\pi}\oint_i \ln(d_2/D_2)\,d\eta, \tag{2.6}$$

where

$$d_n = [(x_n - \xi)^2 + (y_n - \eta)^2]^{1/2}, D_n = [(x_n - \xi)^2 + (y_n + \eta + 2w)^2]^{1/2}, n = 1, 2 \tag{2.6a}$$

and the subscripts "o" and "i" are associated with clockwise integrations of the outer and the inner fronts, respectively. Since there are four unknowns x_1, x_2, y_1, y_2 with four equations (2.3)–(2.6), the system is closed.

b. Formulation of the quasi-geostrophic, one-and-a-half-layer model

In a similar fashion to the barotropic case, we now consider the eddy-wall collisions in a quasi-geostrophic, one-and-a-half-layer model. In this case, the governing equation is the potential vorticity equation:

$$\nabla^2\psi - \gamma^2\psi = \begin{cases} q_1 & 0 \le r < 1 \text{ (interior)} \\ q_2 & 1 \le r < b \text{ (annulus)} \\ 0 & b \le r < \infty \text{ (outside)}, \end{cases} \tag{2.7}$$

where ψ is the nondimensional interfacial displacement anomaly measured positively downward, γ is the ratio of the eddy's length scale to the Rossby radius, q_1 and q_2 are the constant potential vorticity anomalies for the interior and the annulus, and b is the initial outer front radius. The boundary condition is the same as condition (2.2).

The solution satisfying (2.2) and (2.7) is similar to that in (2.3)–(2.6), except that the logarithmic function (ln) is replaced by the modified Bessel function of order

zero and a minus sign ($-K_0$). The solution consists of four equations with four unknowns related to the front positions $[x_1(t), y_1(t)]$ and $[x_2(t), y_2(t)]$:

$$\frac{dx_1}{dt} = \frac{q_2}{2\pi}\oint_o [-K_0(\gamma d_1) - K_0(\gamma D_1)]\, d\xi + \frac{q_1 - q_2}{2\pi}\oint_i [-K_0(\gamma d_1) - K_0(\gamma D_1)]\, d\xi \quad (2.8)$$

$$\frac{dx_2}{dt} = \frac{q_2}{2\pi}\oint_o [-K_0(\gamma d_2) - K_0(\gamma D_2)]\, d\xi + \frac{q_1 - q_2}{2\pi}\oint_i [-K_0(\gamma d_2) - K_0(\gamma D_2)]\, d\xi \quad (2.9)$$

$$\frac{dy_1}{dt} = \frac{q_2}{2\pi}\oint_o [-K_0(\gamma d_1) + K_0(\gamma D_1)]\, d\eta + \frac{q_1 - q_2}{2\pi}\oint_i [-K_0(\gamma d_1) + K_0(\gamma D_1)]\, d\eta \quad (2.10)$$

$$\frac{dy_2}{dt} = \frac{q_2}{2\pi}\oint_o [-K_0(\gamma d_2) + K_0(\gamma D_2)]\, d\eta + \frac{q_1 - q_2}{2\pi}\oint_i [-K_0(\gamma d_2) + K_0(\gamma D_2)]\, d\eta. \quad (2.11)$$

As before, the subscripts "o" and "i" denote the outer and the inner fronts, respectively. Again, there are four unknowns x_1, x_2, y_1, y_2 with four equations (2.8)–(2.11), so that this system is also closed.

c. Numerical method

By numerically solving the set of coupled, nonlinear equations (2.3)–(2.6) and (2.8)–(2.11), we obtain the temporal evolution of the frontal contours $[x_1(t), y_1(t)]$ and $[x_2(t), y_2(t)]$ for the barotropic model and the one-and-a-half-layer model, respectively. To do so, N_1 and N_2 Lagrangian points are initially placed on the inner and the outer vorticity fronts, respectively. The integral is approximated by the trapezoidal rule, and the differentiation with respect to time is estimated by a second-order Runge-Kutte scheme with a constant time step $\Delta t = 0.1$. In addition, there are several known subroutines to carry out the so-called "surgery procedures." For example, when the Lagrangian points become too sparse or too dense, a subroutine will insert or delete points according to the curvatures of the fronts. The "surgery procedures" also perform tail-clipping, contour-pinching, and contour-splicing if necessary. For more details about these numerical procedures, the reader is referred to Dritschel (1988).

d. Numerical results

In the following two subsections, we first present the numerical results of the barotropic model, and then those of the one-and-a-half-layer model. Earlier studies have shown that, in an open ocean, a barotropic eddy with $b < 2$ is linearly unstable (Flierl, 1988). Therefore, for the barotropic model, we need to check first how a linearly unstable eddy ($b < 2$) evolves along a wall, then independently examine the evolution of a linearly stable eddy ($b > 2$) colliding with a wall. Unfortunately,

however, there is no such stability analysis for an isolated eddy in a "reduced-gravity" one-and-a-half-layer-model. The closest study that we can consider is the above-mentioned study of Flierl (1988) who also examined the stability of an isolated eddy in a two-layer model with the ratio of the upper layer depth to the lower layer depth of 0.19. He found that $b = 2.2$ is the critical value for purely baroclinic disturbance modes 1–3. In view of this, we shall first run a case of $b < 2.2$, and then a case of $b > 2.2$. Before presenting the detailed evolution of the eddy-wall collisions, it is recalled that the evolution of both a barotropic cyclone as well as a quasi-geostrophic cyclone is the mirror image of its anticyclone counterpart. Therefore, it is sufficient to present only a cyclonic (or anticyclonic) evolution.

i. Barotropic model. After the interior vorticity (ω_1) is chosen as 1 or -1, the annulus vorticity (ω_2) is given by $\omega_2 = -\omega_1/(b^2 - 1)$. There are two free parameters that we need to choose: the outer front's radius (b), and the distance between the eddy's center and the wall (w). As mentioned, we shall first examine the evolution of a linearly unstable eddy colliding with a wall, and then examine a linearly stable eddy. It will become clear that an initially stable eddy will first slowly leak the annulus fluid (stage 1) due to the image effect. As the eddy continues to leak, the outer radius of the initially stable eddy will reduce to less than two and it will then become unstable. Next, the annulus fluid rushes quickly out of its parent eddy to form a new ring along the wall (stage 2). It will be seen that the evolution time of the first stage is much longer than that of the second stage.

Linearly unstable eddy-wall collision. Figure 3 shows the evolution of a cyclonic eddy colliding with a wall. In this numerical experiment, $\omega_1 = 1$, $\omega_2 = -0.8$, $b = 1.5$, $w = 1.2$, $N_1 = N_2 = 105$. At $t = 0$, the initially isolated cyclone is cut by the wall. The annulus fluid with an anticyclonic vorticity leaks to the left (looking off-shore) due to the presence of the wall and the image effect. By $t = 20$, a new, small anticyclonic eddy has formed from part of the annulus vorticity. At this stage, the new anticyclonic eddy moves to the left away from the parent eddy along the wall; the area of the new anticyclone (defined as A_n) is 55% of that of the initial annulus (defined as A_a). We also note that as increasingly anticyclonic vorticity accumulates to the left, the interior vorticity is forced to also leak to the left. In the same time, the anticyclonic vortex on the left is advecting the cyclonic interior closer to the wall. Afterward, the cyclonic interior translates to the right due to the image effect. We shall return to this important migration mechanism later.

Another interesting feature is worth mentioning. From $t = 1$ to $t = 12$, an unstable wave with a cyclonic vorticity propagates cyclonically around the inner front and another one with anticyclonic vorticity propagates independently around the outer front. From $t = 12$ and on, the phases of these two waves lock into each other and they begin to interact. This interaction causes both the annulus fluid and the interior fluid to leak to the left.

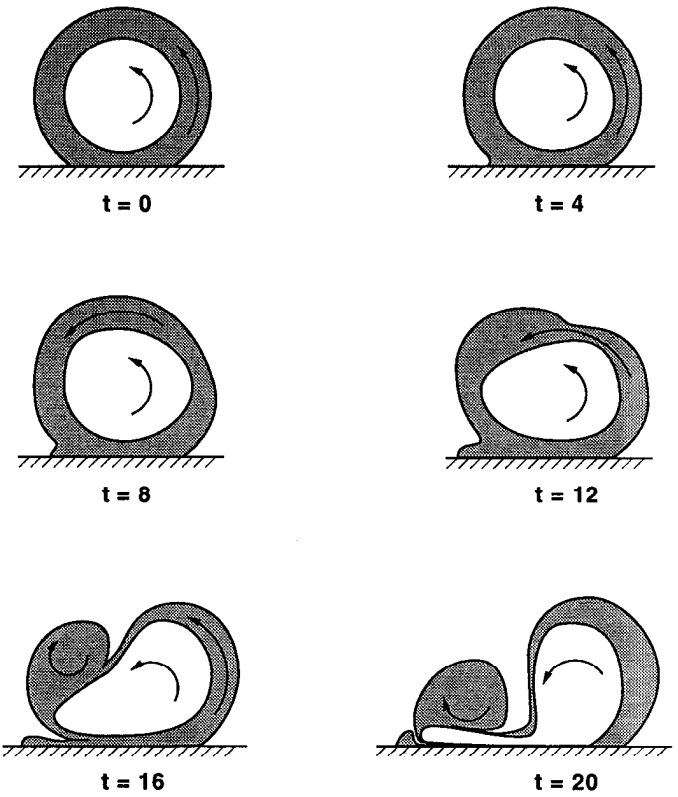

Figure 3. The temporal evolution of the inner and outer fronts of an initially unstable barotropic cyclonic eddy. Both the interior fluid and the annulus fluid leak to the left (looking offshore). The anticyclonic annulus vorticity forms an anticyclonic eddy translating to the left. The parameters are $\omega_1 = 1$, $\omega_2 = -0.8$, $b = 1.5$, $w = 1.2$. Note that the time needed for an interior particle to rotate once is approximately 12.6 (corresponding to $4\pi/\omega_1$). (Traced by hand from original computerized drawings.)

Linearly stable eddy-wall collision. In contrast to the previous case (where the eddy is initially unstable), the present eddy is initially stable. For the case shown in Figure 4, we chose $\omega_1 = 1$, $\omega_2 = -0.19$, $b = 2.5$, $w = 2.1$, and $N_1 = N_2 = 175$. As mentioned, in contrast to the initially unstable eddy case, there are two stages in the present evolution process. In the first stage ($t = 0 - 120$) the stable eddy leaks fluid along a wall (due to the image effect) and the eddy's outer radius decreases (and eventually reduces to less than 2). In the second stage ($t > 120$), the eddy is unstable. The annulus fluid is peeled quickly off the parent eddy because the interior fluid advects the annulus fluid toward the wall. For $t > 160$, a new, large anticyclonic eddy detaches from the parent eddy. This new anticyclonic eddy consists of all the original annulus fluid.

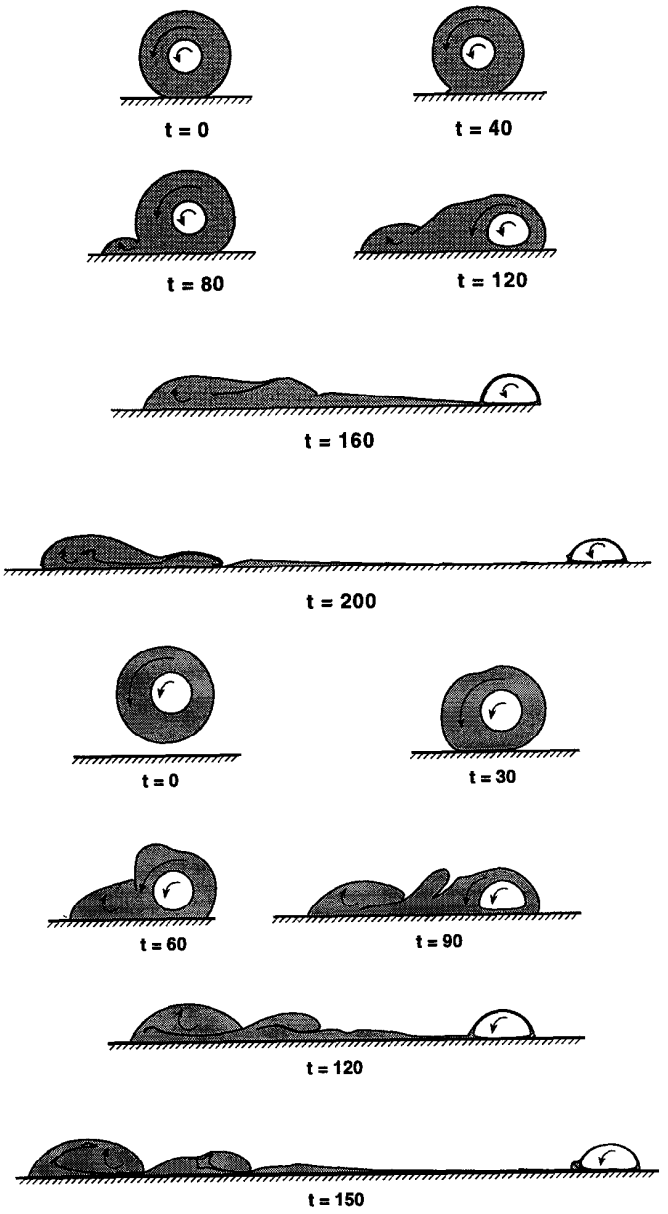
t = 0
t = 40
t = 80
t = 120
t = 160
t = 200
t = 0
t = 30
t = 60
t = 90
t = 120
t = 150

Another important evolution process is that, during the second stage of this eddy-wall collision, the interior of the eddy is forced toward the wall by the leaked vortex on the left. As the interior is continuously forced toward the wall, its shape changes from a circle to a near-semicircle. It moves to the right (whereas the off-spring eddy moves to the left) due to the image effect. As time goes on, the mutual advection of an anticyclone on the left and a cyclone on the right leads both eddies farther toward the wall. Eventually, we see a new anticyclonic eddy on the far left and a cyclonic eddy on the far right. It is also worth pointing out that, during the splitting process, outside fluid slowly intrudes into the new eddy through a streamer.

Note that, in the linearly unstable eddy case, a new eddy has been formed within $t = 20$ (Fig. 3) because the formation process begins immediately after the collision. By contrast, in the originally stable eddy (Fig. 4a), the annulus fluid slowly leaks along the wall from $t = 0$ to $t = 120$ (the first stage), and this gradually causes the originally stable eddy to become unstable. Then, in the second stage a new eddy is formed (from $t = 120$ to $t = 160$). An additional important difference between the two cases is that the new offspring eddy generated from the stable parent eddy (Fig. 4a) is much larger than the new offspring eddy of an unstable parent eddy (Fig. 3). This is so because the volume of the annulus fluid of a stable eddy is initially much greater than that of an unstable eddy.

Three comments should be made before concluding the present discussion. First, the migration speeds of the new offspring eddy and the parent eddy along the wall can be calculated numerically for the case shown in Figure 4a. Such calculations show that, once detached from its parent eddy, the anticyclonic eddy moves to the left at a (nondimensional) constant speed of -0.09, and that the remaining cyclonic core migrates to the right at a (nondimensional) constant speed of 0.27.

We shall, for simplicity, compare the migration of a point vortex (with the same circulation as our eddy) to our vorticity patch. To do so, it is recalled that the point vortex migration speed is given by:

$$C_{pv} = \frac{\Gamma}{4\pi D}, \tag{2.12}$$

Figure 4. (a) The temporal evolution of the inner and outer fronts of an initially stable barotropic cyclonic eddy from $t = 0$ to $t = 200$. As before, the eddy is "cut" by the wall at $t = 0$. The cyclonic eddy leaks its annulus' fluid to the left and the leakage gradually forms an anticyclonic eddy moving to the left (looking offshore). The cyclonic interior of the parent eddy moves toward the wall and migrates steadily to the right. The parameters are $\omega_1 = 1$, $\omega_2 = -0.19$, $b = 2.5$, $w = 2.1$. (Traced by hand from original computerized drawings.) (b) The temporal evolution of the inner and outer fronts of an initially stable barotropic off-center eddy. Here, instead of being cut by the wall (Fig. 4a), the eddy propagates toward the wall. The drift results from the fact that the core is off-center so that the core and rim are mutually advected. Note that there is a remarkable similarity to that in Fig. 4a, indicating that the cut-off process is of a general nature. The parameters are the same as those in Fig. 4a except that $w = 3$ (instead of 2) and the distance between two centers is 0.4 (instead of zero). (Traced by hand from original computerized drawings.)

where Γ is the circulation of the point vortex, D is the point vortex distance to the wall, and the subscript "*pv*" indicates an association with a *point vortex.*

The cyclonic interior with a constant vorticity of unity and a radius of unity has a circulation π. Therefore, we use a point vortex with a circulation of π and a distance to the wall of unity and find that such a point vortex will propagate along the wall at a speed (C_{pv}) of 0.25, which is fairly close to that of our cyclonic interior (0.27). Similarly, the above formula is applied to the detached anticyclonic eddy with a circulation of $-\pi$. The annulus has an approximate area $\pi(b^2 - 1) = 5.25\pi$. If this annulus fluid were to form a circular eddy with the same area as the annulus, then the new eddy's radius would be 2.29. Using this value for D, the anticyclonic point vortex's speed is found to be -0.11, which is also fairly close to the actual speed of -0.09.

The second comment that should be made is that the choice of $\omega_2 = -\omega_1/(b^2 - 1)$ is made so that the isolated eddy will be initially stationary. However, after the eddy is cut off by the wall, the net circulation is slightly greater than zero because part of the eddy has been removed (see Figs. 3 and 4a). To be sure that there is no significant net circulation initially, we calculate numerically the initial area (A_a) of the annulus after the cut-off. We choose $\omega_2 = -\omega_1\pi/(A_a - \pi)$ and rerun the case of Figure 4a with the new value of ω_2. It is found that, even though the detailed transient process is somewhat different from that of Figure 4a, the final state of $\omega_2 = -\omega_1\pi/(A_a - \pi)$ is virtually the same as that of Figure 4a. Namely, all of the annulus fluid is advected along the wall and forms a new eddy. After we carefully compared many other runs of $\omega_2 = -\omega_1/(b^2 - 1)$ with those of $\omega_2 = -\omega_1\pi/(A_a - \pi)$, we concluded that the slight imbalance of the net circulation has a minimum effect on the final state of a new eddy.

Finally, to examine the sensitivity of our results to the initial conditions (involving "cutting" the vortex at $t = 0$), we have also experimented with initially off-centered eddies. Such eddies migrate toward the wall due to the mutual advection of the core and rim. As Figure 4b demonstrates, the results of the two processes are remarkably similar indicating that our process is not sensitive to the initial conditions.

ii. A baroclinic one-and-a-half-layer-model. It is expected that the particle motion of our baroclinic eddy will be slower than that of the barotropic eddy because our baroclinic eddy is quasi-geostrophic. Namely, the time needed for an interior particle to rotate once in the one-and-a-half-layer model should be much longer than that in a barotropic model where the vorticity is comparable to the Coriolis parameter f. This implies that the formation time of a baroclinic off-spring eddy will be longer than that of a barotropic off-spring eddy. For simplicity, after the interior potential vorticity (q_1) is set to be either 1 or -1, the annulus potential vorticity (q_2) is taken to be $q_2 = -q_1/(b^2 - 1)$. We need to choose three free parameters: the outer front's

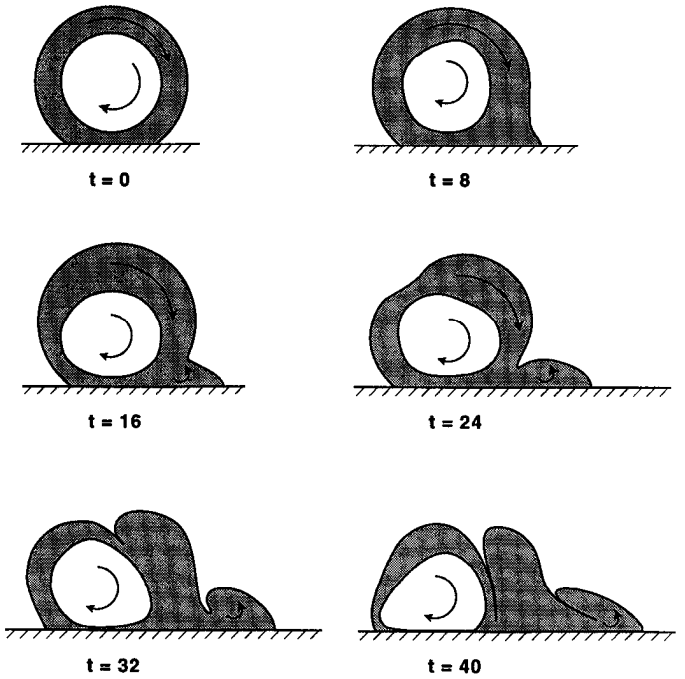

Figure 5. The temporal evolution of the inner and outer fronts of an initially unstable baroclinic anticyclonic eddy. The cyclonic annulus potential vorticity gradually forms a cyclone translating to the right next to the wall. The parameters are $q_1 = -1$, $q_2 = 0.4$, $b = 1.8$, $w = 1.2$, $\gamma = 1$. (Traced by hand from original computerized drawings.)

radius (b), the initial distance between the eddy's center and the wall (w), and the eddy length scale (γ).

Linearly unstable eddy-wall collision. Figure 5 shows the temporal evolution of two potential vorticity fronts associated with an anticyclonic eddy ($q_1 = -1$, $q_2 = 0.4$, $b = 1.8$, $w = 1.2$, $\gamma = 1$, and $N_1 = N_2 = 126$). Similarly to the barotropic cyclonic eddy (Fig. 3), the annulus fluid of the anticyclonic eddy immediately leaks to the right (looking off-shore) due to the wall. As more and more annulus cyclonic potential vorticity is pushed to the right along the wall, a new cyclone is formed on the right (see $t = 40$, for example). By $t = 40$, the area of the new anticyclone (A_n) constitutes about 80% of that of the initial annulus (A_a). As expected, the formation time of this baroclinic eddy is longer than that of the barotropic eddy. It is also noted that the interior is advected toward the wall by the cyclonic vortex on the right. While the interior vortex in the barotropic case leaks along the wall (see Fig. 3), the interior in the baroclinic case does not leak at all. In a similar fashion to the barotropic case, the outside fluid is entrained into the newly formed eddy through a streamer.

Linearly unstable eddy-wall collision. Figure 6 shows the evolution of two potential vorticity fronts for an anticyclonic eddy ($q_1 = -1$, $q_2 = 0.19$, $b = 2.5$, $w = 2.1$, $\gamma = 1$,

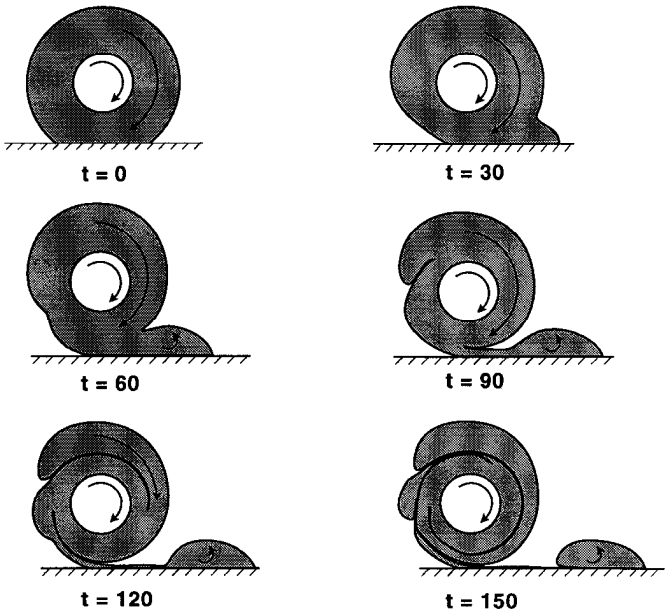

Figure 6. The temporal evolution of the inner and outer fronts of an initially stable barotropic anticyclonic eddy from $t = 0$ to $t = 150$. The anticyclone leaks its annulus' fluid to the right; and the cyclonic annulus fluid gradually forms a cyclone moving to the right (looking offshore). The remaining eddy is stable and approximately stationary. The outside fluid intrudes into the parent eddy through streamers. The parameters are $q_1 = -1$, $q_2 = 0.19$, $b = 2.5$, $w = 2.1$, $\gamma = 1$. (Traced by hand from original computerized drawings.)

and $N_1 = N_2 = 175$). For $t > 0$, the cyclonic annulus begins to leak very slowly to the right. At $t = 120$, we see that only a small portion of the cyclonic annulus potential vorticity has leaked to the right along the wall and that most of the annulus fluid remained around the eddy's core. At $t = 150$, this cyclonic (annulus) along-wall flow generates a small, weak cyclonic eddy moving to the right. The percentage of the area of the new cyclonic eddy relative to that of the initial annulus (after the cut-off) is 14%. Since only a small portion of the annulus fluid leaks out of the parent eddy, the outer radius of the remaining eddy is larger than 2.2. Therefore, the remaining eddy is still stable and stationary which is quite different from the barotropic case where the remaining eddy was unstable. Note that the newly born eddy in the one-and-a-half layer model is much smaller than the one in the barotropic model because the image effect is much smaller. Since interactions of the interior and the newly formed cyclone are weak, the interior is stationary too. As in the barotropic case, the migration speed of the off-spring eddy was numerically calculated. These calculations show its formation, the off-spring eddy migrates at a speed of 0.01. By using the point vortex formula, $C_{pv} = \Gamma k_1(2D)/2\pi$ (see e.g., Pedlosky, 1987), we obtain a speed

Table 1. Calculation of relative areas of newly generated eddies as a function of b and w (corresponding to the linearly stable eddies shown in Figs. 4 and 6).

	Outer radius (b)	Distance to a wall (w)	Eddy's length scale, γ	Relative area of a new eddy (A_n/A_a)
barotropic	2.5	2.4	0	100%
	2.5	2.3	0	100%
	2.5	2.2	0	100%
	2.5	2.1	0	100%
	2.7	2.1	0	100%
	2.9	2.1	0	100%
	3.1	2.1	0	100%
one-and-a-half layer	2.5	1.2	1	80%
	2.5	1.7	1	15%
	2.5	2.1	1	14%
	2.8	2.1	1	15%
	3.1	2.1	1	16%
	2.5	2.1	0.5	4%
	2.5	2.1	0.8	10%
	2.5	2.1	1.5	20%

of 0.011 which agrees well with the above numerical computations. An additional interesting feature is that, as before, the outside fluid wraps around the eddy's core.

e. The role of the three free parameters (b, w and γ)

We shall now examine the sensitivity of the results to the outer radius (b) and the initial distance between the eddy's center and the wall (w). To do so, we shall further study the formation time and the ratio of the area of a new eddy to that of an initial annulus by varying the outer radius (b) and the eddy's initial distance to the wall (w). When $b \to \infty$ (i.e., $\omega_2 = 0$) there is only one front and the eddy is merely translating along the wall due to a nonzero net circulation.

i. A barotropic model. The results of the calculations are listed in Table 1. First, we kept b constant and reran the model with increasing w. We found that, for all of the runs, all the annulus fluid eventually drains out of the parent eddy and forms a new anticyclone to the left (as shown in Fig. 4), even though the transient processes vary from case to case. The formation time of the anticyclone increases as the initial distance to the wall (w) increases. Second, we kept w constant and increased the value of b. Again, we found that, ultimately, all the annulus fluid comes out of the parent eddy, even though the transient processes differ from each other. As the outer radius (b) increases, the formation time decreases.

Table 1 illustrates that in all the cases the annulus fluid eventually detaches from the interior of the eddy to form a new eddy. Note that when $w \geq b$ (i.e., a wall does

not cut an eddy), all the annulus fluid stays with the interior as should be the case. The natural question to ask is whether there is a parameter regime in which $0 < A_n/A_a < 100\%$. To answer this question, we kept $(b - w)$ a constant (0.2) and reran the model varying b from 2 to 3.5 with an increment of 0.1. Our results show that $A_n/A_a = 100\%$ for all of these runs and that the transient processes are very similar to those of Figure 4.

In view of these, the following statements can be made. When a wall cuts off an eddy, the eddy first leaks fluid. This leakage eventually causes the center of the outer front to be displaced away from the center of the inner front, so that it sets up a dipole structure (such as a cyclone to the right and an anticyclone to the left). This type of dipole drifts toward the wall due to the mutual advection of the vortices. When it comes close enough to the wall, the cyclone and the anticyclone separate from each other due to the image effect; the separation intensifies as time goes on. This process is, of course, very different from that of an isolated eddy in an open ocean described by Stern [(1987, see (his) Fig. 8], in which the dipole never separates into two eddies. To verify the effect of such a dipole drift on the eddy splitting process, we ran cases in which an eddy with displaced centers (i.e., the center of the core does not coincide with the center of the outer rim) is initially placed away from the wall. Because of mutual advection the eddy moves toward the wall (Fig. 4b). Ultimately, it splits into two eddies in a manner very similar to that shown in Figures 3 and 4a.

ii. A one-and-a-half-layer-model. Table 1 shows that, as in the barotropic case, for a constant value of b, the relative size of the new eddy (i.e., the ratio of the final area of a new eddy to the area of the initial annulus) increases as the distance to the wall w decreases. In a similar fashion to the barotropic case, it is also found that the formation time of the new eddy increases as the distance to the wall w increases [for a constant outer radius (b)]. For a constant value of w, the relative size of a new eddy increases as the outer radius b increases. On the other hand, for a constant value of w, as b increases, the formation time increases.

The relationship between the eddy's dimensionless length scale (γ) and the size of the newly formed eddy (A_n/A_a) has also been examined (Table 1). It shows that the size of the new eddy increases as γ increases and that the formation time is insensitive to γ.

As in the barotropic case, the one-and-a-half-layer results were verified using a vortex with an off-center core instead of cutting the vortex with a wall. This collision process is again rather similar to that shown in Figures 5 and 6 and, therefore, is not presented.

In summary, five remarks can be made. First, a barotropic eddy leaks fluid along a wall and the leaked fluid causes an initially stable eddy to become unstable. This is not the case, however, with a one-and-a-half-layer model where a stable eddy

remains stable. Second, the eddy interior advects its annulus fluid toward a wall forming a new eddy. Third, after a new eddy is born, both the parent eddy and the off-spring eddy migrate away from each other along the wall. Fourth, advection of the newly formed eddy by the parent eddy and vice versa cause both eddies to move farther into the wall. This causes an increased migration and separation (due to the image effect) which, in turn, reduces the mutual advection (due to the increased distance between the eddies). Fifth, the formation time (i.e., the time required for the eddy generation) for an unstable eddy is much shorter than that needed for a stable eddy. This is the case for both the barotropic model and the one-and-a-half-layer model.

Some of the above dynamics are also present in the simple case of two point vortices of opposite sign situated next to a wall. As in the case of an off-centered eddy (Fig. 4b), such eddies are initially mutually advected toward the wall. Upon reaching the immediate vicinity of the wall they separate and migrate along the wall due to the image effect. For the barotropic case, the velocities of such point vortices has been given by Lamb (1932) in the form,

$$\frac{dx}{dt} = \frac{\Gamma}{4\pi} \frac{x^2}{y(x^2 + y^2)}; \frac{dy}{dt} = \frac{-\Gamma}{4\pi} \frac{y^2}{x(x^2 + y^2)},$$

where, as before, Γ is the intensity of the vortex.

For our slightly more complicated one-and-a-half-layer model, the solution can be written in the form,

$$\psi = \frac{\Gamma}{2\pi} K_0(2x) + \frac{\Gamma}{2\pi} K_0(2y) - \frac{\Gamma}{2\pi} K_0[2(x^2 + y^2)^{1/2}]$$

which gives,

$$\frac{dx}{dt} = \frac{\Gamma}{\pi} \left\{ K_1(2y) - K_1[2(x^2 + y^2)^{1/2}] \frac{y}{(x^2 + y^2)^{1/2}} \right\}$$

$$\frac{dy}{dt} = \frac{-\Gamma}{\pi} \left\{ K_1(2x) - K_1[2(x^2 + y^2)^{1/2}] \frac{y}{(x^2 + y^2)^{1/2}} \right\}$$

and is shown in Figure 7.

3. An isopycnic model of eddy splitting

To verify the new eddy splitting process presented earlier in Section 2, we now use an isopycnic, primitive equation model described in Shi and Nof (1993). As mentioned, this Bleck and Boudra (1986) isopycnic model uses an Eulerian method, whereas the contour dynamics model uses a Lagrangian method. Since the isopycnic model is a primitive equation model, it includes more dynamical processes than are

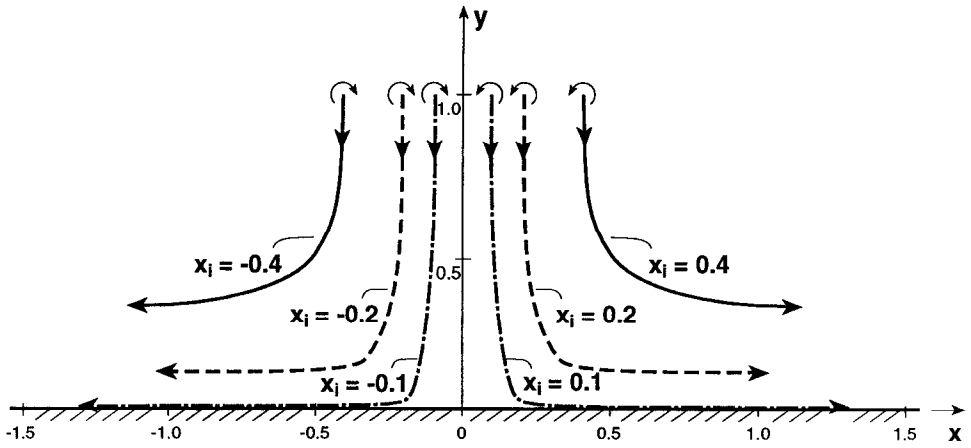

Figure 7. The path of two point vortices (of opposite signs) next to a wall in a one-and-a-half-layer model. Initially, the eddies are mutually advected toward the wall. After sensing the wall, there is migration and separation along the wall due to the image effect.

contained in the contour dynamics model. However, since our contour dynamics theory is quasi-geostrophic, a primitive equation model is not really necessary. We chose this particular primitive equation model merely for convenience. Our runs include processes whose scale is the deformation radius. Furthermore, the Rossby number is small compared to unity so that the processes are close to be in a quasi-geostrophic balance as is the case with our contour dynamics experiments.

The next two subsections illustrate that a weak cyclonic (anticyclonic) eddy will form from an anticyclonic (cyclonic) eddy. In contrast to the previous contour dynamics study (which used both a barotropic and a one-and-a-half-layer model), we use here only a two-layer model with two different initial interfacial displacement profiles. However, we shall take the upper layer thickness to be much thinner than the lower layer thickness, so that this two-layer model works just like a one-and-a-half-layer model. Since the eddy generation process of a constant potential vorticity eddy-wall collision in a one-and-a-half-layer model was just presented, we shall first study this process in an isopycnic model. Then, we shall proceed and present the eddy splitting process of baroclinic, Gaussian eddy-wall collisions. In each of these two cases, we shall illustrate that, similar to a contour dynamics model, the interior vortex advects the annulus vortex toward the wall so that the annulus fluid moves away from the parent eddy to form a new eddy.

a. Collisions of a constant potential vorticity eddy with a wall

To initialize the isopycnic model, we first need to choose a profile of the interfacial displacement anomaly for an eddy in a one-and-a-half-layer model. We chose a solution that is a straightforward extension of Csanady's (1979) solution to an eddy

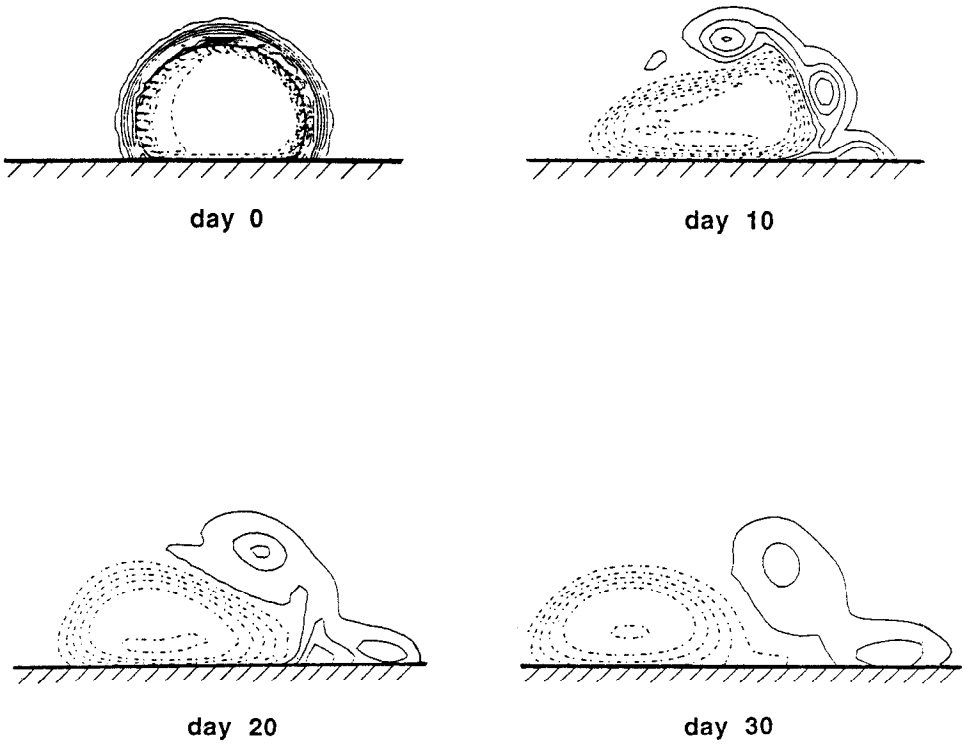

Figure 8. Contours of the potential vorticity anomaly for a violent collision of an anticyclonic eddy with a wall. The annulus fluid is advected anticyclonically to form a weak cyclonic eddy migrating to the right. The original eddy changes into a wodon moving at a constant speed of 4.2 km day^{-1} to the left. The parameters are $H = 1000$ m, $q'_m = 3.2 \times 10^{-8}$ sec^{-1} m^{-1}, $x_c = 510$ km, $y_c = 50$ km, $b_1 = 100$ km, $b_2 = 120$ km. The contour interval is 5×10^{-9} sec^{-1} m^{-1}.

with two piece-wise uniform potential vorticity anomalies: $-H_i/R_d^2$ in the interior region, and $-H_a/R_d^2$ in the annulus region (see Shi, 1992, Appendix B). The additional boundary conditions that we used are that the velocity is continuous across the inner front and zero along the outer front. It can be shown that, under such conditions, $H_iH_a < 0$, i.e., the potential vorticity anomalies change sign as one goes from the interior to the annulus.

Figure 8 illustrates an anticyclonic eddy collision corresponding to such an eddy that is suddenly cut off by a vertical wall. From $t = 0$ day to $t = 20$ days, the interior anticyclonic fluid advects the annulus anticyclonic fluid to the right, and this process is compatible with that of Figure 5. At $t = 10$ days, due to instability of the eddy, the shape of the interior is deformed. On day 20, the cyclonic annulus fluid is pushed farther to the right by both the interior and the image effect. At $t = 30$ days, this anticyclone-wall collision produces a new cyclone to the right along the wall. Similar to the result of the contour dynamics study shown in Figure 5, the newly formed

cyclonic eddy is weak compared to its anticyclonic counterpart. This new, weak, cyclonic eddy moves slowly to the right. The area of the new eddy in Figure 5 is approximately 80% of that of the initial annulus, which is encouragingly close to the final area of the new eddy in Figure 8 (approximately 100% of that of the initial annulus).

Interactions of the interior with the annulus force the interior to move farther into the wall. Then, the initial constant potential vorticity eddy is transformed into a half-circular wodon-like eddy (see e.g., Shi and Nof, 1993). In a similar fashion to the result shown in Figure 5, the present numerical calculation shows that the remaining parent eddy migrates to the left at a constant speed of 4.2 km day^{-1}. By using the wodon solution of Shi and Nof (1993), we obtain an analytical speed of 4.0 km day^{-1}, which agrees well with the numerical calculation. The isopycnic model also shows that eddy-wall collisions generate a Kelvin wave propagating along the wall. Such a wave was, of course, not present in the contour dynamics model because the contour dynamics techniques filters these waves out. Our numerical calculations show that the Kelvin wave carries about 20% of the original anticyclonic mass and energy, and 15% of the initial cyclonic mass and energy.

Since the isopycnic model is a primitive equation model, the evolution of a cyclone is not exactly the mirror image of an anticyclone though, as mentioned, the difference between the two is very small. Figure 9 illustrates contours of the potential vorticity anomaly of a cyclonic eddy collision with a wall. As before, at $t = 0$, the eddy is conceptually cut by the wall; from $t = 0$ to 20 days, the interior gradually advects the annulus fluid to the left. In contrast to Figure 8, Figure 9 illustrates that, at $t = 30$ days, the parent cyclonic eddy generates two new weak anticyclonic eddies to the left along the wall. Note that the interior is first forced toward the wall by the anticyclonic annulus fluid and then is transformed into a wodon. This cyclonic wodon moves to the right at a constant speed of 3.7 km day^{-1}. By using again the wodon speed formula of Shi and Nof (1993) to calculate the wodon-like eddy's migration speed, we obtain a translation speed of 4.0 km day^{-1}, which agrees well with the numerical calculation.

b. Collisions of a Gaussian eddy with a wall

After applying the isopycnic model to re-examine constant potential vorticity eddy-wall collisions, the next question to be asked is whether this eddy generation mechanism depends on the initial profile of the eddy. To answer this question, we used a Gaussian profile (instead of a constant potential vorticity eddy's profile) to initialize the isopycnic model. We have done so for both a cyclone and an anticyclone as the nonlinear evolution is not symmetrical. All of these interactions are virtually indistinguishable from those of the constant potential vorticity eddies (see Shi, 1992, Figs. 21 and 22).

In summary, we can conclude that the results of both the Eulerian method and

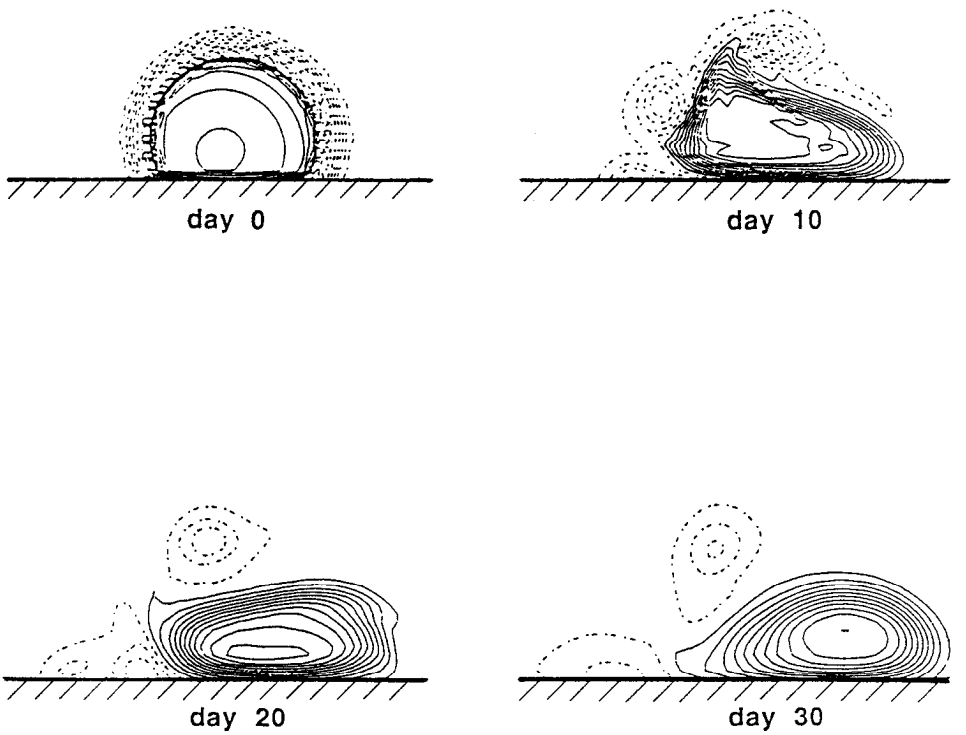

Figure 9. Contours of the potential vorticity anomaly for a cyclonic eddy colliding with a wall. It shows that the annulus fluid is pushed cyclonically to generate a weak anticyclonic eddy migrating to the left. The original eddy changes into a wodon moving at a constant speed of 3.7 km day^{-1} to the left. The parameters are $H = 1000$ m, $q_m' = 5.6 \times 10^{-8}$ sec^{-1} m^{-1}, $x_c = 510$ km, $y_c = 50$ km, $b_1 = 100$ km, $b_2 = 120$ km. The contour interval is 5×10^{-9} sec^{-1} m^{-1}. The similarity between Figures 9 and 8 indicates that, as stated, the flows were close to being quasi-geostrophic. Note, however, that the contours in the two figures are not identical (even though the contour intervals are).

those of the Lagrangian method point to a new eddy splitting mechanism. After studying eddy-wall collisions using an Eulerian method with two different profiles, we can also conclude that this new eddy splitting mechanism is not sensitive to the initial profiles of the interfacial displacement anomaly.

4. Discussion

a. The eddy splitting process

Both the results of the contour dynamics model and the isopycnic model show that violent eddy-wall collisions result in the splitting of the parent eddy into two eddies. During the collision, the interaction of the interior and the off-centered annulus forces the interior and the annulus farther toward the wall via mutual advection. The

resultant final configuration is a cyclonic eddy to the right and an anticyclonic eddy to the left. These results were obtained by using different models (a barotropic contour dynamics model, a one-and-a-half-layer contour dynamics model, and a two-layer isopycnic model with two different initial interfacial displacement profiles), implying that they are of quite general nature.

For convenience, the barotropic eddy splitting process is discussed first. The parent cyclonic eddy has a cyclonic vorticity in the interior and an anticyclonic vorticity in the annulus. When the cyclone collides with the wall, the anticyclonic annulus fluid leaks on the left due to the impossibility of penetrating the wall. As a result, the anticyclonic annulus fluid develops into a new anticyclone on the left. Similarly, an anticyclonic eddy has an anticyclonic vorticity in the interior and a cyclonic vorticity in the annulus. When it collides with the wall, the cyclonic annulus fluid leaks to the right and forms a new cyclone moving to the right along the wall.

During the process of eddy splitting, the new eddy and the parent eddy are pushed farther into the wall via mutual advection. As both the parent eddy and the off-spring eddy move closer to the wall, they translate farther and farther away from each other due to the image effect. Consequently, one always sees an anticyclone translating to the left and a cyclone moving to the right. The increased distance between the eddies causes, in turn, a reduction in the eddies' mutual advection and the drift toward the wall. A very similar eddy splitting process can be described for the one-and-a-half-layer model eddy. The only meaningful difference between the barotropic and baroclinic case is that the leakage and the new off-spring eddy are smaller in the baroclinic case.

The above results agree with the laboratory experiments of Agnon (1986) who, using a rotating tank, generated an intensive cyclonic vortex near the vertical wall. He showed that the cyclonic eddy leaks fluid forming an inertial jet to the left of the eddy. The inertial jet formed an anticyclonic eddy to the left of the parent eddy along the wall, as predicted by our models.

b. Comparison with oceanic observations

Clearly, a detailed comparison of our models with observations is impossible at this stage because of the simplifications in our model (e.g., the neglect of friction which allows the use of images) and the limited available data. Therefore, we shall only attempt to perform a qualitative comparison.

One of the most comprehensive surveys of eddy-wall collisions is that of Vidal *et al.* (1992) who examined Loop Current rings. They identified the collision from temperature, salinity, and dynamic topography distributions. As suggested by our models, they found that, when the anticyclonic eddy collided with the continental slope, the eddy translated to the left (looking onshore). During the collision process, the anticyclonic ring shed approximately one third of its volume to the right. They also found that a cyclonic ring was formed to the *right* of the parent ring as suggested by

our model. Because of the relatively large amount of mass that was lost from the parent eddy, we speculate that the actual collision was similar to our collision processes, all of which have, in general, been termed "violent" collisions.

While the above observations compare favorably with our model, the following data do not necessarily support our model predictions. Vukovich and Waddell (1991) used data from XBT/hydrographic cruises in the Gulf of Mexico and from satellite images to study collisions of a warm-core ring with the western slope. They indicated that the collisions of the anticyclonic ring with the continental slope induced a large-scale flow to the left in the upper layer near the slope. There was a cyclonic ring to the *left* of the Loop current warm-core ring along the slope. The line-up is the cyclone to the left and the anticyclone to the right, which is different from both our model results and the observations of Vidal *et al.* (1992). We speculate that the cyclonic ring of Vukovich and Waddell (1991) could have been generated by shelf water being pushed to deep regions by the anticyclonic ring. This process is, of course, absent from our analysis as our boundaries were taken to be vertical.

c. Concluding remarks

A barotropic contour dynamics model, a one-and-a-half-layer contour dynamics model, and a two-layer isopycnic primitive equation model were used to examine the eddy's collisions with a wall. The primary aim was to investigate the detailed temporal evolution of "violent" eddy-wall collisions which result from a strong advective current or another vortex that forces the eddy toward the wall. This violent process is conceptually represented by abruptly slicing the eddy. It should be distinguished from "gentle" interactions caused by the variations of the Coriolis parameter with latitudes which slowly advect the eddies toward western boundaries (Shi and Nof, 1993). The results are summarized as follows:

1) As the studies which have examined "gentle" eddy-wall collisions have shown, due to the image effect, the cyclonic eddy leaks fluid to the left (Figs. 3, 4 and 9) while the anticyclonic eddy leaks fluid to the right (Figs. 5, 6 and 8). However, in contrast to gentle collisions which are associated merely with relatively small leakages (Shi and Nof, 1993), violent collisions cause the parent eddy to leak excessively and to split into two parts.

2) Violent collisions of a cyclonic eddy with a wall generate an anticyclonic ring (Figs. 3, 4 and 9), while violent collisions of an anticyclonic ring with a wall generate a cyclonic ring (Figs. 5, 6 and 8).

3) Violent eddy-wall collisions always lead to an anticyclone on the left and a cyclone on the right. Mutual interactions of the resulting cyclone and anticyclone advect both eddies farther toward the wall. They separate farther and farther away from each other due to an intensification of the image effect. The

increased distance between the eddies causes, in turn, a reduction in their mutual advection toward the wall.

4) During violent eddy-wall collisions, the outside fluid either intrudes into the new offspring eddy (Figs. 3, 4 and 5) or wraps around the parent eddy's core (Fig. 6) through the generation of filaments.

The above theory was applied to various rings in the real ocean. We found that our model predictions qualitatively agreed with some observations but disagreed with others. Possible explanations for the disagreement were discussed.

Acknowledgments. Comments by M. E. Stern, W. K. Dewar and S. Meacham were very helpful. Glenn Flierl and R. Mied gave us advice during the early stages of this work. This study was supported by Office of Naval Research grant N00014-89-J-1606 and by National Science Foundation grants OCE-9012114 and OCE-9102025. This paper constitutes a part of Shi's Ph.D. dissertation and is partially supported by a postdoctoral fellowship of the University of Maryland Center for Environmental and Estuarine Studies, Horn Point Environmental Laboratory.

REFERENCES

Agnon, Y. 1986. The lives of an eddy—experimental study of planetary eddies. 1986 Summer Study Program in Geophysical Fluid Dynamics. WHOI, WHOI-86-45, 180–191.

Berk, H. and K. Roberts. 1970. The water-bag model. Meth. Comp. Phys., *9,* 87–134.

Bleck, R. and D. Boudra. 1986. Wind-driven spin-up in eddy-resolving ocean models formulated in isopycnic and isobaric coordinates. J. Geophys. Res., *91,* 7611–7621.

Csanady, G. 1979. The birth and death of a warm-core ring. J. Geophys. Res., *84,* 777–780.

Dritschel, D. 1988. Contour surgery: a topological reconnection scheme for extended integrations using contour dynamics. J. Comp. Phys., *77,* 240–266.

Dorofeyev, V. and V. Larichev. 1992. The exchange of fluid mass between quasi-geostrophic and ageostrophic motions during the reflection of Rossby waves from a coast. I. The case of unbounded ocean. Dyn. Atmos. Oceans, *16,* 305–329.

Flierl, G. 1988. On the instability of geostrophic vortices. J. Fluid Mech., *197,* 349–388.

Lamb, H. 1932. Hydrodynamics. Dover, New York, 738 pp.

Minato, S. 1982. Geostrophic adjustment near the coast. J. Oceanogr. Soc. Japan, *38,* 225–235.

—— 1983. Geostrophic response near the coast. J. Oceanogr. Soc. Japan, *39,* 141–149.

Nof, D., 1988a. Draining vortices. Geophys. Astrophys. Fluid Dyn., *42,* 187–208.

—— 1988b. Eddy-wall interactions. J. Mar. Res., *46,* 527–555.

Pedlosky, J. 1987. Geophysical Fluid Dynamics. Springer-Verlag, New York, 710 pp.

Shi, C. 1992. The migration and generation of oceanic eddies along western boundaries. Ph.D. dissertation, The Florida State University, 96 pp.

Shi, C. and D. Nof. 1993. The destruction of lenses and generation of wodons. J. Phys. Oceanogr., (in press).

Stern, M. 1986. On the amplification of convergences in coastal currents and the formation of "squirts." J. Mar. Res., *44,* 403–421.

—— 1987. Horizontal entrainment and detrainment in large-scale eddies. J. Phys. Oceanogr., *17,* 1688–1695.

—— 1989. Evolution of locally unstable shear flow near a wall or a coast. J. Fluid Mech., *198,* 79–99.

Stern, M. and L. Pratt. 1985. Dynamics of vorticity fronts. J. Phys. Oceanogr., *17,* 1688–1695.
Umatani, S. and T. Yamagata. 1987. Evolution of an isolated eddy near a coast and its relevance to the "Kyucho." J. Oceanogr. Soc. Japan, *43,* 197–203.
Vidal, V., F. Vidal and J. Perez-Molero. 1992. Collision of a Loop Current anticyclonic ring against the continental shelf slope of the western Gulf of Mexico. J. Geophys. Res., *97,* 2155–2172.
Vukovich, F. and E. Waddell. 1991. Interactions of a warm ring with the western slope in the Gulf of Mexico. J. Phys. Oceanogr., *21,* 1062–1074.
Zabusky, N., M. Hughes and K. Roberts. 1979. Contour dynamics for equations in two dimensions. J. Comp. Phys., *30,* 96–106.

Received: *4 March, 1993;* revised: *10 August, 1993.*